REPORT 1386

INVESTIGATION OF THE DRAG OF VARIOUS AXIALLY SYMMETRIC NOSE SHAPES OF FINENESS RATIO 3 FOR MACH NUMBERS FROM 1.24 TO 7.4 [1]

By Edward W. Perkins, Leland H. Jorgensen, and Simon C. Sommer

SUMMARY

Drag measurements have been made at zero angle of attack for a series of fineness ratio 3 nose shapes. The models included various theoretically derived minimum drag shapes, hemispherically blunted cones, and other more common profiles. Pressure-distribution measurements for a series of hemispherically blunted cones were also obtained. The Mach number and Reynolds number ranges of the test were 1.24 to 7.4 and 1.0×10^6 to 7.5×10^6 (based on model length), respectively.

Of the models tested, the paraboloid of revolution had the least foredrag below a Mach number of 1.5, and the theoretically minimum drag shape for a given length and diameter based upon Newton's impact theory had the least foredrag above a Mach number of 1.5. The theoretical shapes for minimum pressure drag for the auxiliary conditions of given length and diameter or given diameter and volume derived by von Kármán and by Haack do not have less drag than all other possible shapes having identical values of the same parameters. No model had the least foredrag for the complete Mach number range. Wherever possible, theoretical values of the foredrag based upon the sum of the theoretical skin-friction drag and the theoretical wave drag were calculated for comparison with the experimental results.

The results for the series of hemispherically blunted cones have important practical significance since it was found that the diameter of the hemispherical tip may be fairly large without markedly increasing the foredrag over that of a sharp pointed cone of the same fineness ratio. In fact, for a fixed fineness ratio of 3, the foredrag is reduced somewhat by a small degree of blunting, although for a fixed cone angle blunting always increased the drag. An empirical expression, applicable for free-stream Mach numbers greater than 2, is developed for calculating the wave drag of the series of hemispherically blunted cones.

INTRODUCTION

The allied problems of predicting the drag of bodies of revolution and of minimizing the drag by proper shaping of the body have been the objects of numerous theoretical investigations. With regard to the problem of predicting the drag, that part of the drag which has thus far proved most amenable to theoretical calculation is the wave drag. For pointed bodies of revolution at Mach numbers sufficiently high for shock-wave attachment, the wave drag may be calculated by either perturbation theory or by the method of characteristics. For highly blunted nose shapes there is no simple theoretical method for predicting the pressure distribution and drag. Therefore experimental results have been relied upon for this information.

The first part of the present investigation is a study of the pressure distribution and drag of a series of hemispherically blunted cones. Although it might seem that the use of such a blunt nose would result in a high drag penalty, preliminary estimates [2] have indicated that the drag of a nose shape consisting of a hemispherical surface faired into an expanding conical surface can be less than that of a sharp cone of the same length-to-diameter ratio. The results of preliminary estimates of the variation of drag with the ratio of hemispherical tip diameter to base diameter for fineness ratio 3 have indicated that a small reduction in drag can be realized at all supersonic Mach numbers. Perhaps more important than the reduction in drag is the indication that a relatively large hemispherical tip can be used without incurring any drag increase above that of a sharp-nosed cone of the same fineness ratio. In order to verify these predictions and to provide quantitative drag data the present investigation was undertaken.

The second phase of the investigation is a study of minimum drag nose shapes. Most theoretical approaches have been directed toward the mimimization of the wave drag only. Von Kármán (ref. 1) developed an integral equation for the wave drag of slender bodies of revolution at moderate Mach numbers. Using this equation, he derived a minimum drag nose shape (commonly referred to as the Kármán ogive) for a given length and diameter. Subsequently, Haack (ref. 2) and others (refs. 3 and 4) have used the Kármán integral equation in developing minimum drag shapes for other auxiliary conditions, such as given length and volume or given volume and diameter. Through the use of the Kármán

[2] These preliminary estimates were made by summing the experimentally determined wave drag of the hemispherical nose and the theoretical pressure drag of the conical afterbody, assuming that the pressure on the surface of the conical afterbody was the same as that for a sharp cone of the same slope.

[1] Supersedes NACA Research Memorandum A52H28 by Edward W. Perkins and Leland H. Jorgensen, 1952, and NACA Research Memorandum A52B13 by Simon C. Sommer and James A. Stark, 1952.

526507—60——80

integral equation as the basis for these derivations, the apparently unnecessary yet simplifying assumption of zero slope of the meridian at the base has been imposed. This restriction is pointed out by Ward in reference 5, wherein he shows that his more general expression for wave drag reduces to that obtained by von Kármán for the special case of a body having zero slope at the base. In a later paper (ref. 6) Ferrari developed a minimum drag nose shape for a given length and diameter which has a finite slope of the meridian at the base. For the high supersonic Mach number range, minimum drag shapes based upon Newton's law of resistance have been derived by Eggers, Resnikoff, and Dennis (ref. 7). These shapes differ appreciably from comparable optimum shapes for low supersonic Mach numbers, although the theoretical optimum shapes in both instances have blunt noses when the length is fixed and sharp noses when the length is allowed to vary.

Due to the basic assumptions in the derivation of the Kármán integral equation, it may be expected that the shapes resulting from the use of this equation are theoretically optimum from a minimum drag standpoint only for large fineness ratios and low supersonic Mach numbers. In contrast, the shapes resulting from the Newtonian theory may be expected to be optimum only at high supersonic Mach numbers. However, for low fineness ratio shapes at moderate Mach numbers, it is impossible to say a priori which of the theoretically optimum shapes will have the lesser wave drag, or in fact if either of the theories is capable of predicting the least-drag profile. One of the purposes of the present investigation is, therefore, to compare the experimental drags of these theoretically optimum shapes and of other more common profiles for an intermediate fineness ratio over a wide Mach number range. To this end a series of fineness ratio 3 models of these theoretically optimum shapes have been tested in the Mach number range from 1.24 to 3.67.

SYMBOLS

A model base area, sq in.

C_D total drag coefficient, $\frac{\text{total drag}}{qA}$

C_{D_F} foredrag coefficient based on base area, $\frac{\text{total drag—base drag}}{qA}$

C'_{D_F} foredrag coefficient based on volume to the $\frac{2}{3}$ power, $\frac{\text{total drag—base drag}}{qV^{2/3}}$

C_{D_W} wave drag coefficient, $\frac{\text{wave drag}}{qA}$

d hemisphere diameter, in.

D model base diameter, in.

K similarity parameter, $\frac{M}{L/D}$

L model length, in.

M free-stream Mach number

P pressure coefficient, $\frac{p_t-p}{q}$

P_t pitot-pressure coefficient, $\frac{p_t-p}{q}$

P_ω cone pressure coefficient, $\frac{p_\omega-p}{q}$

p_l local static pressure, lb/sq in.

p free-stream static pressure, lb/sq in.

p_t pitot total-head pressure, lb/sq in.

p_ω cone static pressure, lb/sq in.

q free-stream dynamic pressure, $\frac{\gamma}{2}pM^2$, lb/sq in.

r model local radius, in.

R model base radius, in.

Re free-stream Reynolds number based on body length

V model volume, cu in.

X axial distance from the nose, in.

α angle of attack, deg

γ ratio of specific heats of air, taken as 1.40

θ circumferential angle of hemisphere measured from the upstream stagnation point, deg

ω cone half angle, deg

APPARATUS AND TESTS

The experimental investigation was conducted in three facilities, the Ames 1- by 3-foot supersonic wind tunnels No. 1 and No. 2, and the Ames supersonic free-flight wind tunnel. The two 1- by 3-foot wind tunnels are conventional tunnels which are equipped with flexible top and bottom plates for varying the test section Mach number.

For the tests in the supersonic free-flight tunnel the models were launched from a smooth-bore 20mm gun, and were supported in the gun by plastic sabots. Separation of the model from the sabot was achieved by a muzzle constriction which retarded the sabot and allowed the model to proceed in free flight through the test section of the wind tunnel. A more detailed description of this facility is given in reference 8.

MODELS

Sketches of the models tested, including dimensions, specified parameters, and defining equations, are presented in figure 1. For the series of hemispherically blunted cones shown in figure 1(a) the length-to-diameter ratio of 3 is constant, and the cone angle is decreased as the bluntness (ratio of hemisphere diameter to base diameter) is increased. For the series in figure 1(b) the base diameter and cone angle are constant, and the length decreases with increase in bluntness.

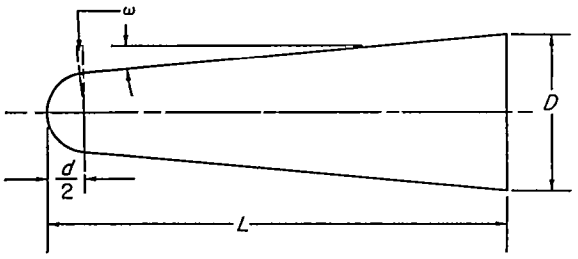

Model no	$\frac{d}{D}$	ω	D
1	0	9°28'	1.75
1f	0	9°28'	0.45
2	.075	8°52'	1.75
2f	.075	8°52'	0.45
3	.150	8°15'	1.75
3f	.150	8°15'	0.45
4	.300	6°59'	1.75
4f	.300	6°59'	0.45
4p	.300	6°59'	2.00
5	.500	5°10'	1.75
5f	.500	5°10'	0.45
5p	.500	5°10'	2.00
6p	1.000	0	4.00

Note: 4p, 5p, and 6p are pressure distribution models. Models 1f through 5f, are free-flight models.

(a)

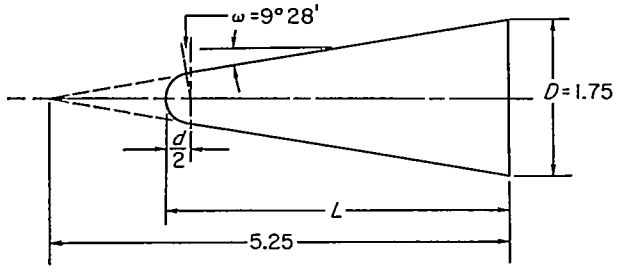

Model no	$\frac{d}{D}$	$\frac{L}{D}$
1	0	3.00
7	.075	2.81
8	.150	2.62
9	.300	2.24

(b)

(a) Hemisphere-cone series for constant $\frac{L}{D}=3$.

(b) Hemisphere-cone series for constant cone angle.

FIGURE 1.—Model profiles. (Dimensions are in inches.)

The family of fineness ratio 3 models defined by the equation $r=R(X/L)^n$ is shown in figure 1(c). For length and base diameter specified, the profiles of the hypersonic optimum (Newtonian) nose and the nose developed by Ferrari (ref. 6) can both be very closely approximated by the above equation for n=¾. (See fig. 2.) Since the ¾-power nose is a reasonable approximation to these theoretically derived optimum shapes, it alone has been tested and is referred to throughout the report as the hypersonic optimum nose.

Fineness ratio 3 models of the minimum drag shapes based upon the work of von Kármán and subsequently Haack are shown in figure 1(d). For any two specified parameters such as length and diameter, length and volume, or diameter and volume, these are the theoretical optimum nose shapes and for convenience have been designated as the *L-D*, *L-V*, and *D-V* Haack noses. A similar designation has been used for the circular-arc tangent ogive and cone shown in figure 1(e). The *L-V* ogive has the same length and volume as the *L-V* Haack model, and the *D-V* cone has the same diameter and volume as the *D-V* Haack model. Also shown in figure 1(e) is a fineness-ratio-3 ellipsoid.

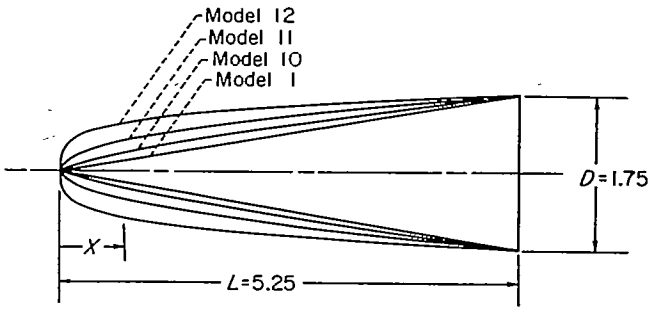

Model no	Designation	n
1	Cone	1
10	Hypersonic opt.	3/4
11	Paraboloid	1/2
12	1/4 Power	1/4

(c)

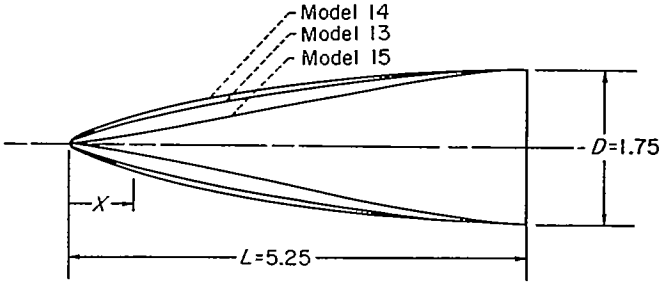

Model no	Designation	Specified parameters	c
13	*L-D* Haack	Length, dia.	0
14	*L-V* Haack	Length, vol.	1/3
15	*D-V* Haack	Dia, vol.	-2/3

(d)

(c) Profile defined by $r=R\left(\frac{X}{L}\right)^n$

(d) Haack minimum drag noses defined by $r=\frac{R}{\sqrt{\pi}}\sqrt{\varphi-\frac{1}{2}\sin 2\varphi+c\sin^3\varphi}$,

$$\varphi=\text{arc cos}\left(1-\frac{2X}{L}\right).$$

FIGURE 1.—Continued.

Except for the pressure-distribution models, all the nose shapes were constructed of duralumin. The 30- and 50-percent hemispherically blunted cone pressure-distribution models (models 4p and 5p) were cast of tin and bismuth, and the hemisphere-cylinder pressure-distribution model (model 6p) was constructed of steel.

TESTS

Wind tunnels No. 1 and No. 2.—The total drag was measured by means of a strain-gage balance located in the model support housing. The base pressure was determined through the use of a liquid manometer connected to two holes in the supporting sting at the base of the model. Experimental values of foredrag were then taken as the difference between

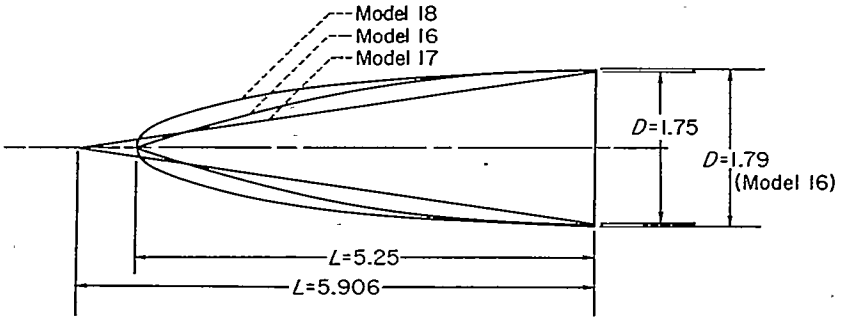

Model no	Designation	$\frac{L}{D}$
16	L-V Ogive	2.93
17	D-V Cone	3.38
18	Ellipsoid	3

(e)

(e) Other profiles.

FIGURE 1.—Concluded.

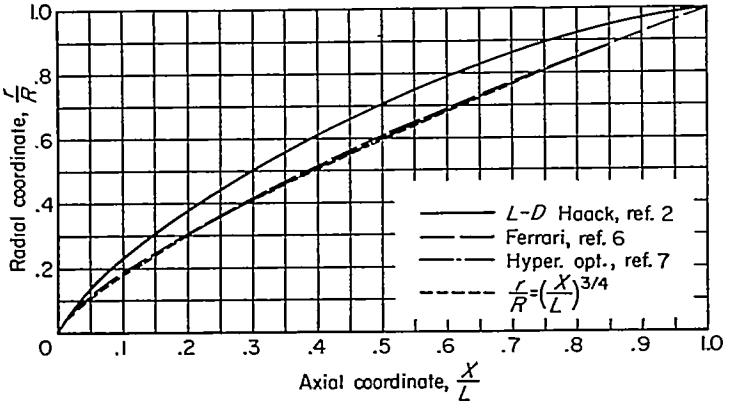

FIGURE 2.—Comparison of profiles of minimum drag noses for given length and base diameter.

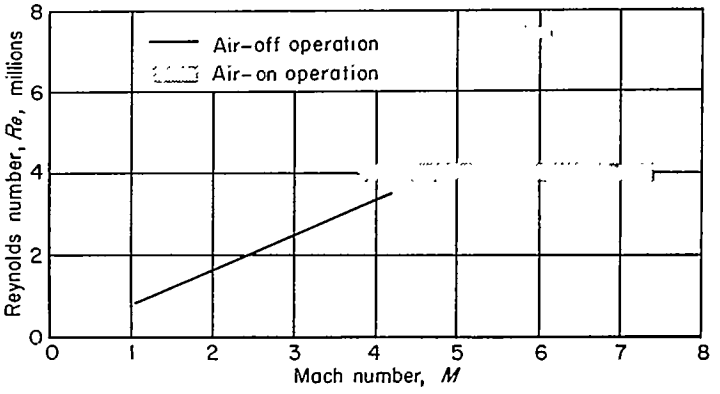

FIGURE 3.—Range of Mach numbers and Reynolds numbers of tests in the Ames supersonic free flight wind tunnel.

the measured total drag and base pressure drag. Because of the operating characteristics of the tunnels, it was not possible to maintain a constant Reynolds number throughout the Mach number range of 1.24 to 3.67; however, an attempt was made to keep the Reynolds number constant for all models at each Mach number. In the following table the average Reynolds number (based on model length) and its limit of variation for all models tested at each Mach number are listed:

M	$Re\times10^{-6}$	Tunnel No.
1.24	2.42±0.14	1
1.44	1.17±0.01	1
	3.14±0.20	
1.54	4.10±0.10	2
1.96	4.14±0.12	2
1.99	2.01±0.01	1
2.86	4.00±0.10	2
3.06	4.00±0.19	2
3.67	3.45±0.07	2

The pressure-distribution tests were all made in tunnel No. 2 at Mach numbers of 1.5, 2, 3, and 3.7 and at an average Reynolds number of about 4×10^6. Pressure distributions for the hemisphere-cone pressure models (models 4p, 5p, and 6p) were determined through the use of a liquid manometer system connected to two rows of orifices along the models and spaced 180° apart. The models were rotated and a longitudinal pressure distribution at each 30° increment in circumferential angle was obtained. The resulting pressure coefficients at each longitudinal station were averaged to obtain the values presented.

Free-flight wind tunnel.—With no air flow through the wind tunnel, Mach numbers varied from 1.2 to 4.2, depending on the model launching velocity. This condition is referred to as "air off." Reynolds number varied linearly with Mach number from 1.0×10^6 to 3.3×10^6, as shown in figure 3. With air flow established in the wind tunnel, referred to as "air on," the combined velocities of the model and Mach number 2 air stream, with the reduced speed of sound in the test section, provided test Mach numbers from 3.8 to 7.4. In this region of testing, Reynolds number was held approximately at 4×10^6 by controlling test-section static pressure. In addition, some models were tested at approximate Reynolds numbers of 3×10^6 at Mach number 6.

Drag coefficient was obtained by recording the time-distance history of the flight of the model with the aid of a chronograph and four shadowgraph stations at 5-foot intervals along the test section. From these data, deceleration was computed and converted to drag coefficient. This report includes only the data from models which had maximum observed angles of attack of less than 3°, since larger angles measurably increased the drag.

ANALYSIS OF DATA

REDUCTION OF DATA

All the experimental data have been reduced to coefficient form and the data from wind tunnels Nos. 1 and 2 have been corrected for the effects of the small nonuniformities in the wind-tunnel flow. The free-stream static-pressure variations in the model-free tunnel have been applied as corrections to the drag and pressure-distribution data by simple linear superposition. Corrections due to the effects of stream-angle variation were well within the limits of accuracy of the data and have therefore been neglected. No corrections were necessary for the data obtained in the free-flight tunnel.

PRECISION

The uncertainty of the experimental data from tunnels No. 1 and No. 2 was calculated by considering the possible errors in the individual measurements which entered into the determination of the stream characteristics, pressure distributions, and drag. The final uncertainty in a quantity was taken as the square root of the sum of the squares of the possible errors in the individual measurements. The resulting uncertainties in the final quantities are as follows:

Quantity	Uncertainty
P	± 0.004
C_{D_F}	± 0.004
α	$\pm 0.15°$

The variation of the free-stream Mach number over the length of each model tested was less than ± 0.01 for all test Mach numbers. The uncertainty in the Mach number at a given point in the stream is ± 0.003.

The magnitude of the calculated uncertainty in the drag coefficient appears rather large relative to the observed scatter of the data. Drag coefficients for repeated tests generally agreed within ± 0.002. It is therefore believed that the drags of models relative to one another are sufficiently accurate for comparative purposes, although the absolute magnitudes of the drag coefficients for the models at a particular Mach number may be in error by the magnitude of the uncertainty.

Since there are no known systematic errors in the data from the free-flight tunnel, the accuracy of the results is indicated by the repeatability of the data. Examination of these data shows that repeat firings of similar models under almost identical conditions of Reynolds number and Mach number yielded results for which the average deviation from the faired curve was 1 percent and the maximum deviation was 4 percent.

THEORETICAL CONSIDERATIONS

WAVE DRAG

With the exception of some of the very bluntest models (models 11, 12, and 18) the wave drag of each model was either calculated by theoretical methods or was estimated from existing experimental results. Values for the wave drag of the cone and the tangent ogive were obtained from the exact Taylor-Maccoll theory (refs. 9 and 10) and the method of characteristics (ref. 11), respectively. For the theoretical optimum nose shapes the second-order theory of Van Dyke was used. The exact procedure employed in using the second-order theory was that given in reference 12, in which the approximate boundary conditions at the body surface are used in the calculation of the perturbation velocities, and the exact pressure relation is used to evaluate the pressure coefficients.[3] The method presented therein is strictly applicable to sharp-nosed bodies of revolution at Mach numbers less than that at which the Mach cone becomes tangent to the model vertex. Since the theoretical optimum nose shapes for which the length is fixed (models 10, 13, and 14) have infinite slopes at their vertices (yet may be considered sharp for most practical purposes), an approximation to the shape at the vertex was made to enable use of the theory. The blunt tip was replaced by a short conical section tangent to the original contour. The cone angle, and hence the point of tangency, was selected so that the cone half-angle did not exceed 94 percent of the Mach angle. In the subsequent integrations for the wave drag from the resulting pressure distributions, the data were plotted as rP versus r so that the curves could be smoothly faired through the origin.

A simple method of estimating the wave drag of the hemispherically blunted conical noses has been suggested. It has been proposed that the wave drag of the hemispherical tip, which could be obtained from existing experimental data, be added to the pressure drag of the conical portion of the nose, based upon the assumption that the pressure on the conical surface would be the same as on a pointed cone of the same slope. Hence, the pressure drag of the conical portion of the nose could be obtained by exact theory.

The following empirical expression, based upon certain of the experimental results, is suggested for calculating the wave drag of the hemispherical tip for Mach numbers of 2 and greater:

$$C_{D_W}=\frac{2P_t-1}{3} \tag{1}$$

where P_t is the pitot-pressure coefficient at the tip of the hemisphere which may be calculated with the aid of Rayleigh's equation. This expression was obtained from the results of the pressure-distribution tests, and its derivation is discussed in more detail in the section of the report which is concerned with the pressure-distribution tests. When this expression is used for the wave drag coefficient of the hemispherical portion, the expression for the wave drag coefficient of the complete model for Mach numbers of 2 and greater becomes

$$C_{D_W}=\left(\frac{d}{D}\right)^2\left(\frac{2P_t-1}{3}-P_\omega\right)+P_\omega \tag{2}$$

where P_ω is the surface pressure coefficient or pressure drag coefficient (refs. 9 or 10) for a cone of half apex angle ω at the free-stream Mach number. An approximate expression for ω which is sufficiently accurate for the drag estimates is

$$\omega \cong \tan^{-1}\left[\frac{1-(d/D)}{2(L/D)-(d/D)}\right] \tag{3}$$

FOREDRAG

Values of the foredrag have been calculated by the addition of the estimated or theoretical wave drag and the theoretical

[3] In the application of this method a first-order solution is necessarily obtained.

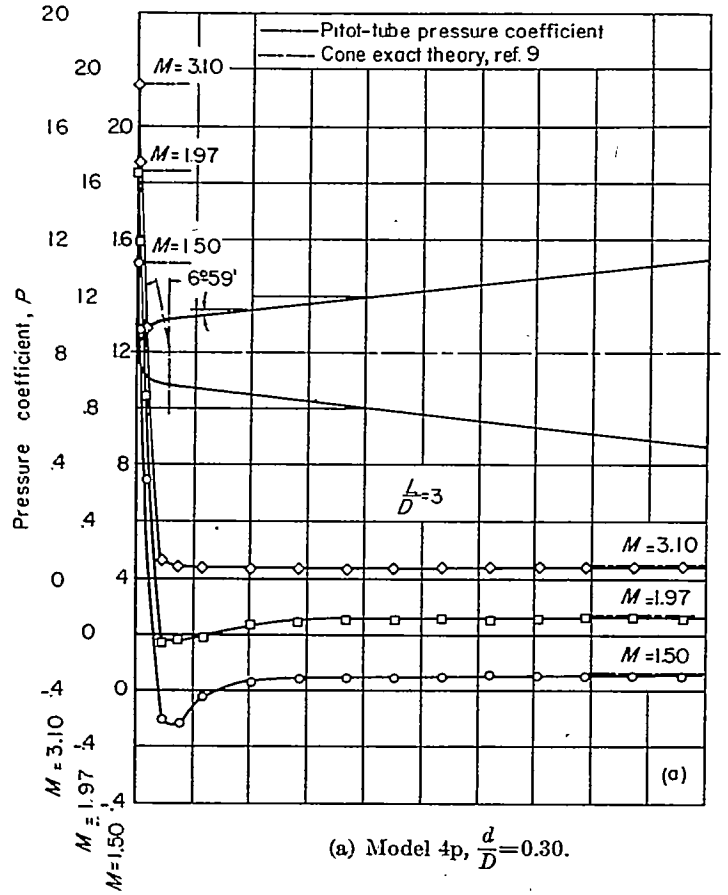

(a) Model 4p, $\frac{d}{D}$=0.30.

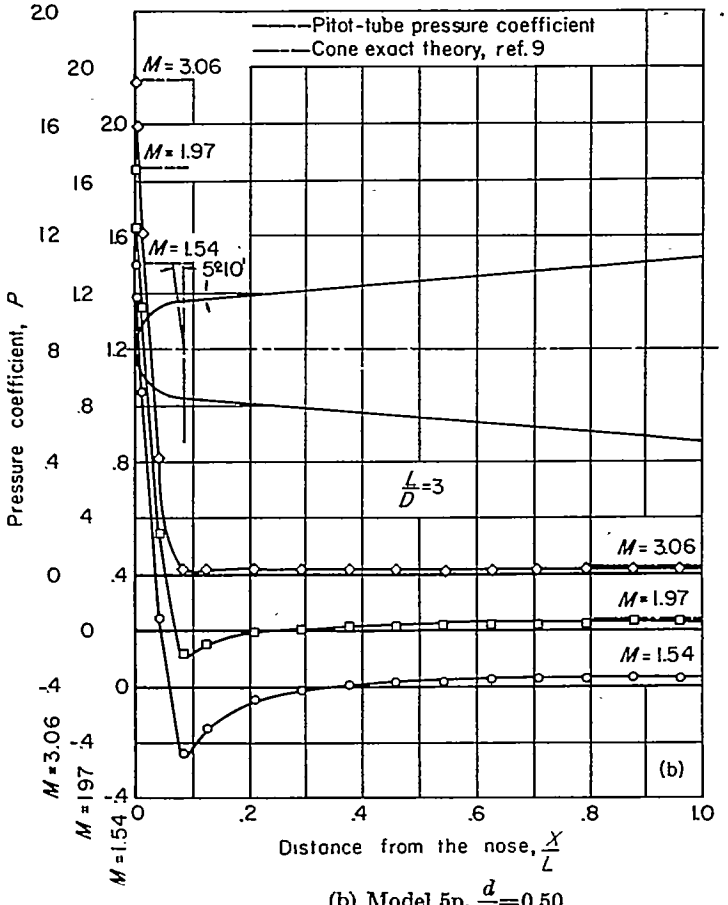

(b) Model 5p, $\frac{d}{D}$=0.50.

FIGURE 4.—Longitudinal distribution of pressure coefficient for hemisphere-cones at 0° angle of attack.

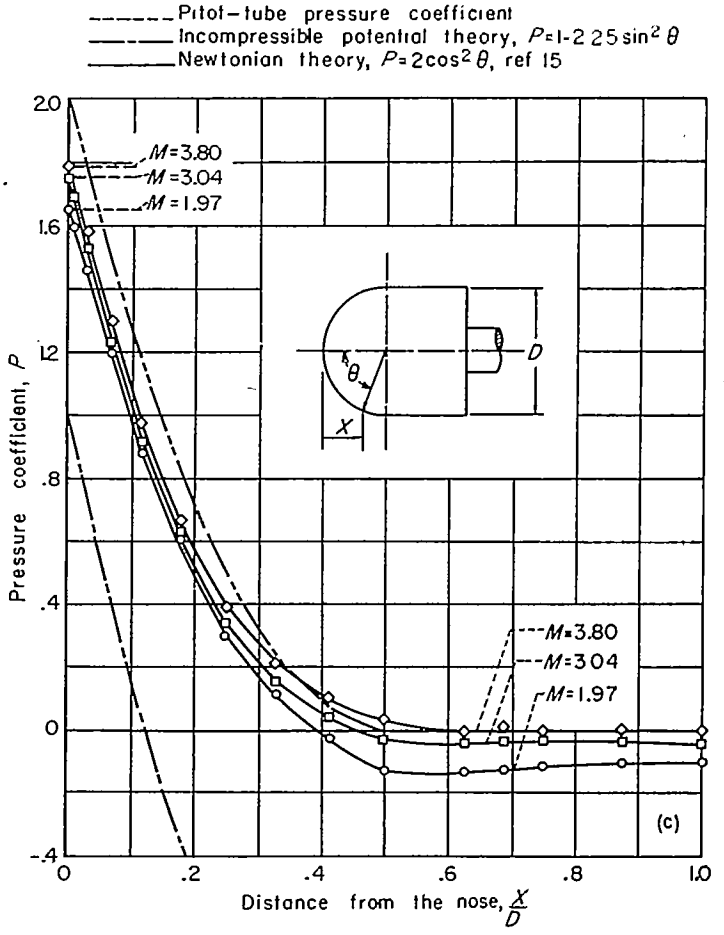

(c) Model 6p, $\frac{d}{D}$=1.00

FIGURE 4.—Concluded.

skin-friction drag. Since the skin-friction drag for laminar-boundary-layer flow contributes so little to the foredrag, the inclusion of the small effects of body shape and compressibility on the skin-friction drag was not considered justified. Therefore, the laminar-skin-friction drag coefficients were calculated by the Blasius formula for flat-plate incompressible boundary-layer flow (ref. 13). For the estimates of the skin-friction drag for turbulent-boundary-layer flow, the body shape effects were neglected, but the effect of compressibility was evaluated by means of the interpolation formula of reference 14 which is based upon an extended Frankl and Voishel analysis.

RESULTS AND DISCUSSION

HEMISPHERICALLY BLUNTED CONES

Pressure distributions.—The pressure-distribution data obtained for models 4p, 5p, and 6p at Mach numbers between 1.5 and 3.8 are shown in figure 4. The data are referred to the free-stream Mach number ahead of the normal shock wave at the nose of each model. Although these Mach numbers were approximately the same for each model, they differed slightly because of the differences in positions of the models within the test section. For each of the models, the pressure coefficient at the nose agrees with the pitot-pressure coefficient calculated by Rayleigh's

equation and shown for comparison by the dashed lines. For models 4p and 5p at Mach numbers 1.97 and 1.5 (figs. 4 (a) and 4(b)) the rapid expansion of the flow over the hemispherical tip is followed by a recompression over the forward part of the conical portion of the nose. The pressure on the conical surface recovers to, or almost to, the theoretical value of the pressure coefficient for a sharp-nosed cone of the same slope. For a Mach number of 3.1, the expanding flow on the hemisphere does not reach a lower pressure than the theoretical surface pressure for a cone of the same slope as the conical afterbody, and it is found that the pressure is constant over most of the conical portion of the nose. From these data it appears that the assumption made in the drag estimates, namely, that the pressure over the conical portion of the nose is constant and equal to the theoretical value for a sharp-nosed cone of the same slope, is essentially correct for free-stream Mach numbers of 3 and greater. For Mach numbers less than 3 the average pressure over the conical section is less than that assumed in the estimates, and hence the estimated drag contribution from this part of the nose will be too high.

A more detailed study of the pressure distribution over the hemispherical portion of this type body is available from the data of figure 4(c). For comparison with these experimental data, the theoretical incompressible distribution (only part of which is shown for simplicity) and the distribution predicted by Newtonian theory (ref. 15) are shown. It is apparent that as the Mach number is increased the pressure distribution approaches that predicted by Newtonian theory. In spite of this trend, it is evident that the distribution would never agree exactly with the Newtonian because the peak pressure coefficient at the nose would be somewhat less than the Newtonian value of 2. An additional factor which has been neglected in the Newtonian theory is the effect of centrifugal forces which, although negligible for the lower Mach numbers, would tend to reduce the theoretical pressure coefficients over the hemisphere in the high Mach number range.

The study of the comparisons of the experimental pressure distributions for the hemisphere with that predicted by Newtonian theory (fig. 4(c)) indicates that an empirical expression for the pressure distribution, which yields reasonably accurate values of the wave drag, may be written. The development of the expression is based upon two experimental results: First, the pressure at the tip of the hemisphere is the stagnation pressure and may be calculated exactly from the Rayleigh equation. Second, at the high Mach numbers the subsequent expansion of the flow is similar to that predicted by Newtonian theory, and the local pressure differs from the Newtonian value by an amount which varies approximately as the cosine of the angle θ. Based upon these observations the following empirical expression for the pressure distribution on a hemisphere may be written:

$$P=2\cos^2\theta-(2-P_t)\cos\theta \qquad (4)$$

where P_t is the pitot-pressure coefficient at the stagnation point on the hemisphere. The expression predicts a pressure coefficient that is exact at $\theta=0$ and agrees with the Newtonian value of $P=0$ at $\theta=90°$. It is apparent from the data of figure 4(c) that, although the resulting pressure distribution will closely approximate the experimental distribution at high Mach numbers, the predicted pressures near $\theta=90°$ will be considerably in error for lower Mach numbers. However, this should not result in a serious error in the pressure drag, since the surface slope is small in this region, and thus the resulting drag contribution is also small. A simple expression for the wave drag coefficient of the hemisphere results from this empirical equation for the pressure distribution. Thus, based upon the maximum cross-section area,

$$C_{D_W}=\frac{2P_t-1}{3} \qquad (1)$$

Values computed from this equation are compared in figure 5 with estimates of the wave drag from total drag measure-

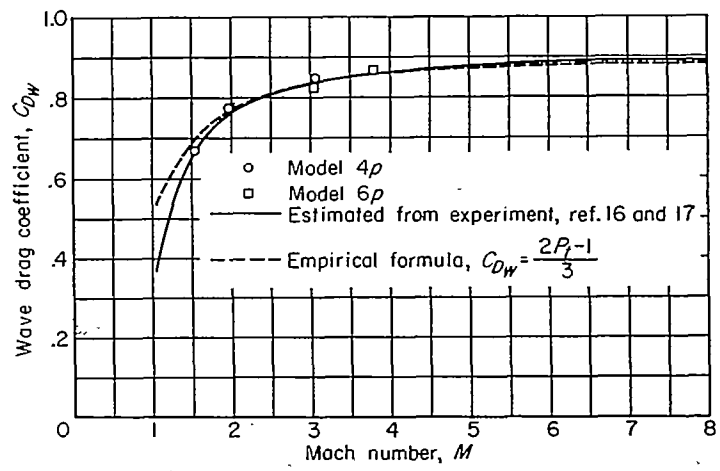

FIGURE 5.—Variation of wave drag coefficient with Mach number for a hemisphere.

ments (refs. 16 and 17) and with the experimental pressure drag determined from the pressure distributions of figure 4. For Mach numbers between 2 and 8 the agreement is excellent. As would be expected from the pressure-distribution results, the values from the empirical expression are too large in the lower Mach number range.

From these data it appears that for the estimates of the wave drag of the hemispherically blunted cones, the contribution of the hemispherical tip to the total wave drag at Mach numbers of 2 and greater may be calculated accurately with the proposed empirical expression.

Flow field.—The recompression of the flow over the upstream portion of the conical afterbody, which was noted previously in the discussion of the pressure distributions, is associated with the appearance, a short distance downstream from the bow wave, of an approximately conical shock wave in the flow field. The schlieren pictures for model 5 (fig. 6) are typical for all the hemispherically blunted cones (models 1 through 5) throughout the Mach number range These pictures show that the intensity of the wave decreases with increasing Mach number. At Mach number 3.06 the wave is no longer evident within the bounds of the schlieren field. The decrease in intensity of the wave is in accord with the changes found in the pressure distribution data.

(a) $M=1.24$

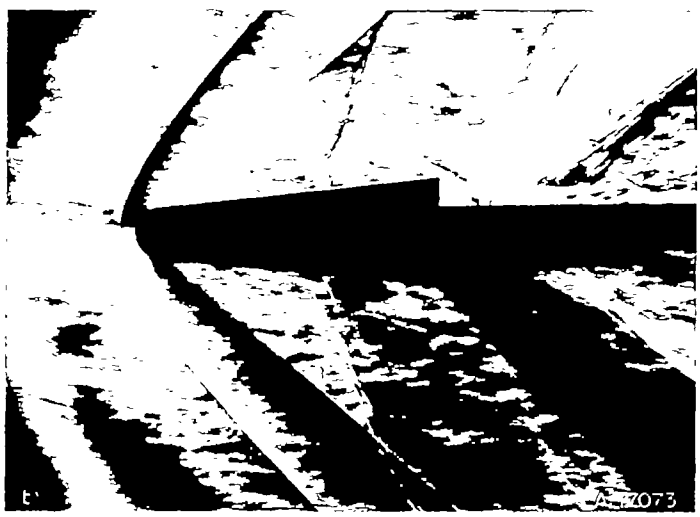

(b) $M=1.54$

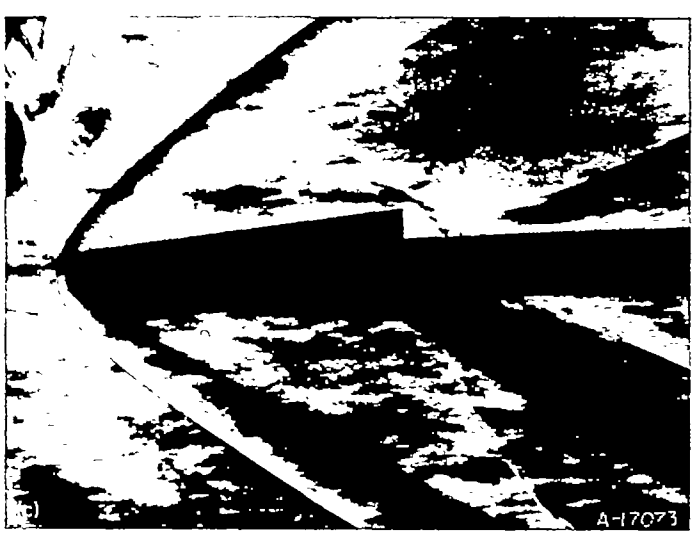

(c) $M=1.96$

FIGURE 6.—Schlieren pictures for 50-percent hemispherically blunted cone, model 5, at various Mach numbers.

(d) $M=3.06$

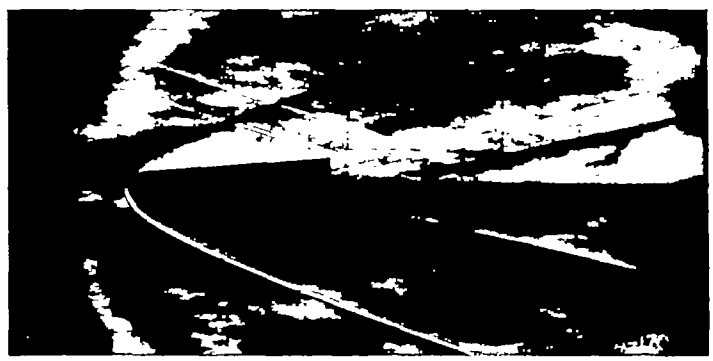

(e) $M=3.67$

Figure 6.—Concluded.

(See fig. 4.) At first glance it might appear that this wave could be associated with a region of separated flow on the hemispherical tip, with subsequent reattachment accompanied by a shock wave. However, the schlieren pictures show no evidence of flow separation. Additionally, it is apparent from the schlieren pictures that this shock wave does not extend from the outer flow down to the body surface but appears to be diffused near the surface. These observations lead to the speculation that the origin of the wave must be associated with the transonic or mixed type of flow which occurs in the vicinity of the nose of the body.

The mechanism by which the compression wave is formed may be much the same as that discussed in reference 18 for the two-dimensional flow around a sharp-nosed double-wedge airfoil section with detached bow wave. It is believed that the wave results from a coalescence of weak compression waves reflected from the body surface. (The existence of the compression region is confirmed by the pressure-distribution data.) These waves apparently originate as expansion waves from the body surface downstream from the sonic point. As indicated in the sketch, these expansion waves which travel along characteristic lines are reflected from the sonic line and the bow wave as compression waves which are in turn reflected from the body surface. The reflection of these wavelets from the body surface occurs in such a manner that they coalesce to form a shock wave.

The dependence of this phenomenon on both the free-stream Mach number and the inclination of the body surface just downstream of the point of tangency of the hemisphere

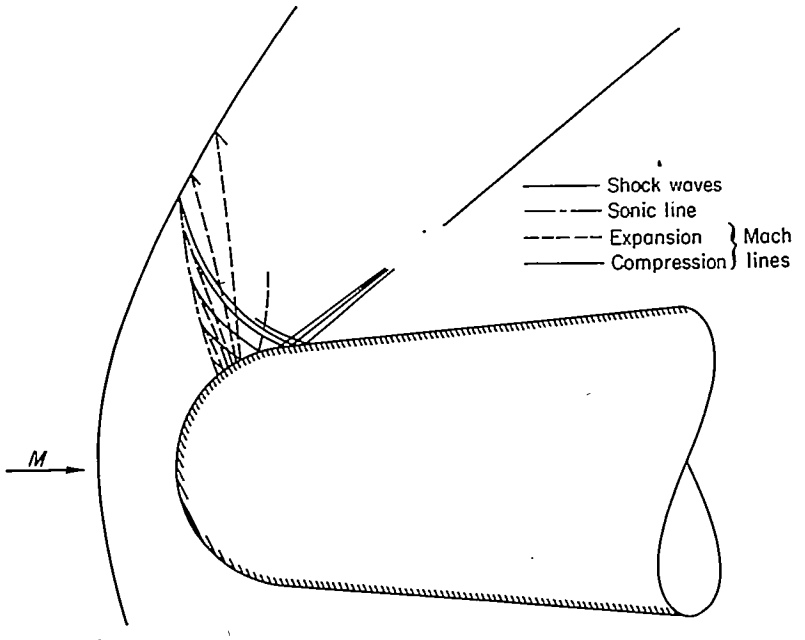

with the afterbody is demonstrated by the following observations. For the hemispherically blunted cones, neither the shock wave nor the region of recompression on the body surface was found for Mach numbers above 3.06. The disappearance of this shock wave and region of compression results from the combination of the movement of the bow wave closer to the body surface and the small upstream movement of the sonic point with increasing Mach number. These changes reduce the extent of the mixed flow region so that for Mach numbers above approximately 3 most of the compression wavelets reflected from the sonic line and bow wave are incident upon the body surface in the expansion region between the sonic point and the point of tangency of the hemisphere with the afterbody and hence are canceled. The importance of the inclination of the body surface in the region of the reflections is indicated by the fact that, although the pressure-distribution data for model 6p (fig. 4(c)) show that at the lowest test Mach number there exists a region of recompression just downstream from the juncture of the hemisphere and cylindrical afterbody, the magnitude of the recompression is very small and does not result in a secondary shock wave that can be detected in the schlieren pictures.

Drag.—The variation of drag coefficient with Mach number for the hemispherically blunted cones of fineness ratio 3 (models 1 through 5) are presented in figure 7. Because of the differences in test technique, the data from the wind tunnels and from the free-flight facility are presented separately. Since the models vary progressively from the sharp-nosed cone to the very blunt model with the large hemispherical tip ($d/D=0.5$), the variation of the foredrag coefficient with Mach number (fig. 7(a)) changes progressively from the familiar variation for a cone (foredrag coefficient decreases with increasing Mach number) to the variation characteristic of a hemisphere (fig. 5). Variation with Mach number of the total drag coefficient (fig. 7(b))[4] is similar for all models in that the drag coefficient continually decreased with increasing Mach number.

The data from figure 7(a) are replotted in figure 8 to show the variation of foredrag with nose bluntness at constant Mach numbers and provide comparisons with the estimated foredrag characteristics. For this series of fineness ratio 3 noses, a small saving in foredrag may be achieved through the use of a hemispherically blunted cone in place of a sharp cone of the same fineness ratio. Perhaps more important is the fact that a relatively large increase in volume over that of a sharp-nosed cone may be realized without incurring any increase in foredrag. An additional factor to be considered is that the hemispherical nose provides an ideal housing for search radar gear. These data show that with increasing Mach number there is a decrease in both the degree of blunting which results in minimum foredrag as well as the maximum blunting allowable such that the foredrag is not greater than that of the sharp-nosed cone. These results are in essential agreement with the preliminary foredrag estimates.

Although the results (fig. 8) show that for this fineness ratio 3 series of models there is some drag reduction with increase in bluntness, the magnitude of the possible drag reduction which is obtainable by this method of blunting decreases rapidly with increasing fineness ratio. In fact, there appears to be an upper limit to the fineness ratio for which this type of blunting will yield any drag reduction. Some indications of the magnitude of this limiting fineness ratio which varies with Mach number have been obtained by comparing the variation with fineness ratio of the estimated wave drag of the $d/D=0.075$ model with that of a cone of the same fineness ratio at Mach numbers of 2 and 3. These results (fig. 9) indicate that the wave drag of the cone is less than that of this moderately blunt model for length-to-diameter ratios in excess of approximately 5.4 and 5.0 at Mach numbers of 2 and 3, respectively. These results also show that the range of nose fineness ratios for which

[4] No attempt has been made to join the air-off data and air-on data because of the differences in Reynolds number, recovery temperature, and stream turbulence.

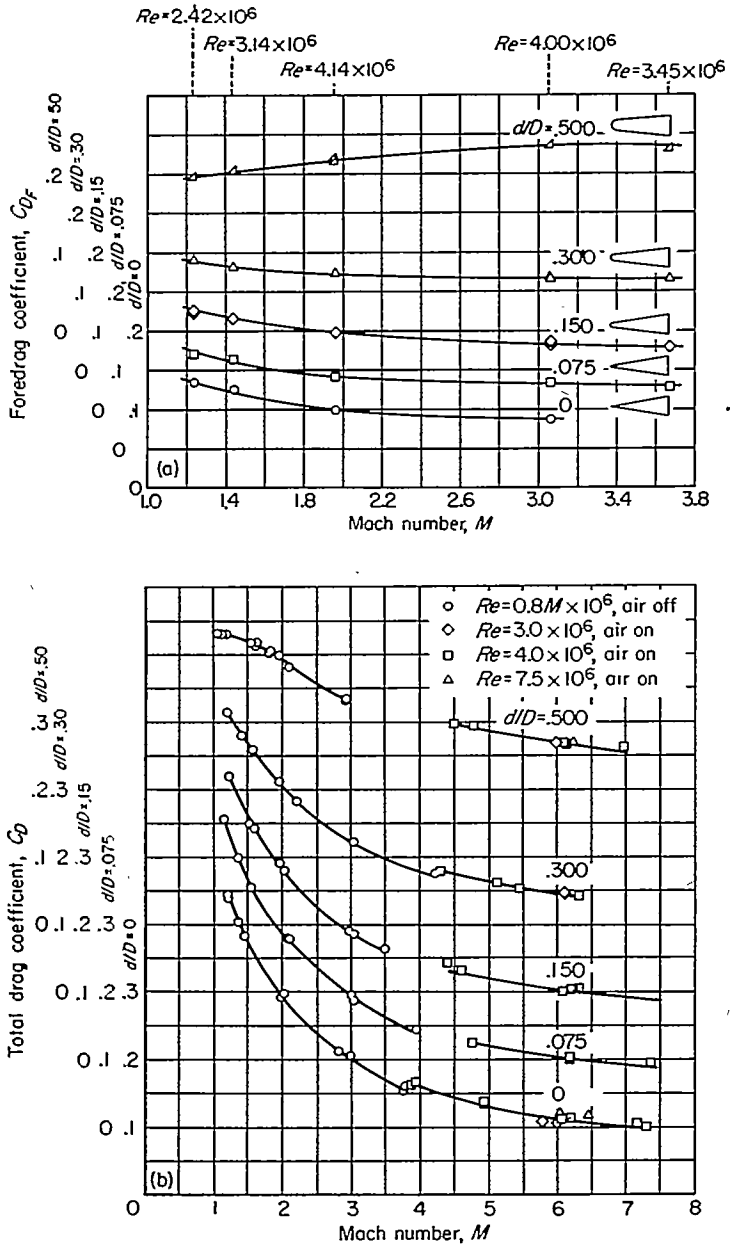

(a) Wind tunnel results.
(b) Free-flight results.

FIGURE 7.—Variation of drag coefficient with Mach number for hemisphere-cone series, constant $\frac{L}{D}=3$.

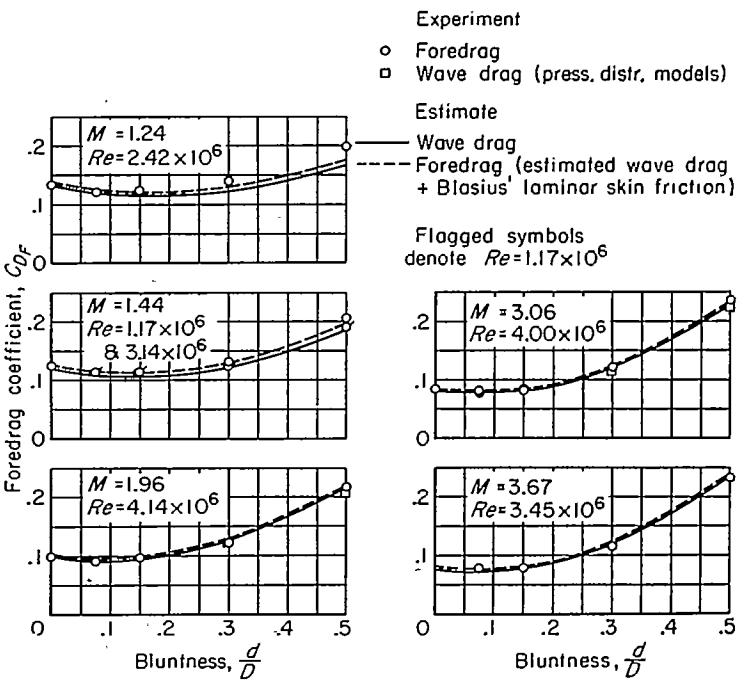

FIGURE 8.—Variation of foredrag coefficient with bluntness for hemisphere-cone series, constant $\frac{L}{D}=3$.

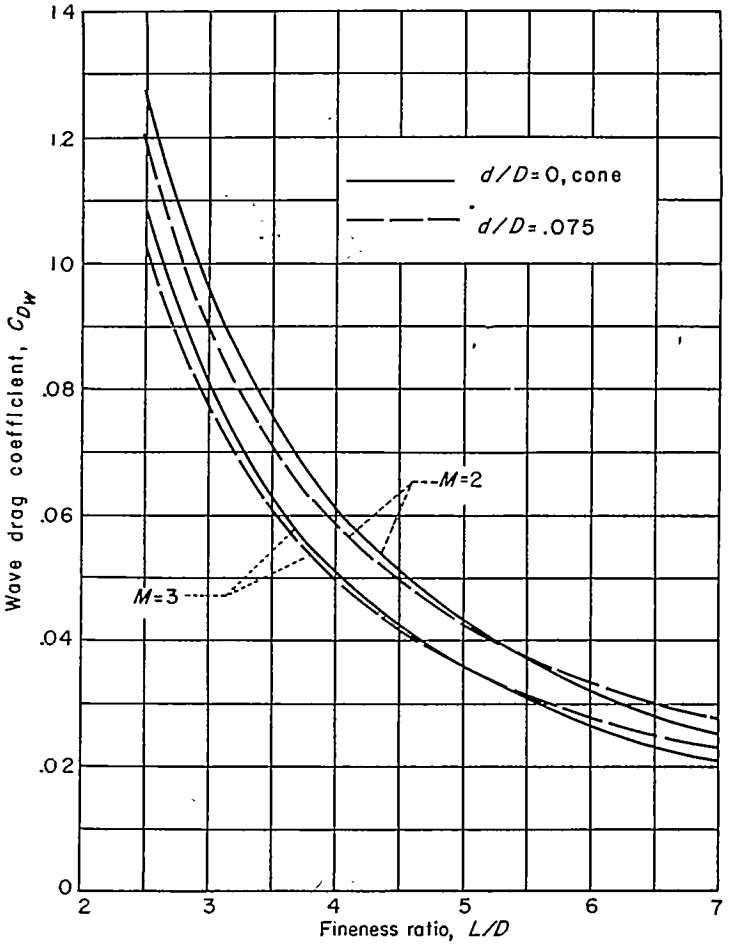

FIGURE 9.—Comparison of the estimated wave drag variation with fineness ratio for a sharp-pointed cone and a 7.5-percent hemispherically blunted cone at Mach numbers 2 and 3.

this type of blunting would be advantageous decreases with increasing Mach numbers.

It should also be pointed out that the drag penalty associated with the use of excessive blunting increases rapidly with increasing fineness ratio. At a Mach number of about 3.1 the data of the present report (fig. 8) indicate that the foredrag coefficient of a 20-percent blunt cone is about 0.01 greater than that of the sharp-nosed cone of the same fineness ratio. This increment represents approximately a 12-percent increase in foredrag and may be compared with the data of reference 19, wherein it is shown that the same degree of blunting for a fineness ratio 8 body results in an increment in wave drag coefficient of 0.053, corresponding to an increase in pressure drag of more than 300 percent.

The estimated wave drag coefficients for the $d/D=0.30$

and 0.50 models at Mach numbers of 3.06 and 1.96 are in very good agreement with the wave drag determined from the pressure distribution models (see fig. 8). Similarly the agreement between the experimental foredrag and the estimated foredrag based upon the estimated wave drag plus laminar incompressible skin-friction drag is very good for Mach numbers 1.96, 3.06, and 3.67. For the tests at these Mach numbers the schlieren pictures taken during the tests indicated that the boundary layer was completely laminar over each of the models. An interesting effect of body shape upon boundary-layer transition is indicated by the results of the tests at $M=1.44$ and 1.24. From the schlieren pictures and the foredrag data it was evident that turbulent boundary-layer flow existed on part of the conical afterbodies of the $d/D=0.30$ and $d/D=0.50$ bodies for the higher Reynolds number at $M=1.44$ and 1.24. In contrast, the boundary-layer flow was laminar over the entire surface of the cone for the identical test conditions. It is believed that the difference between the results for the cone and the blunt bodies results largely from the effects of the differences in body pressure distributions. For the cone the pressure is constant along the surface and therefore neutral insofar as its effect on the boundary-layer flow is concerned. For both the blunt bodies at the low Mach numbers, the pressure gradient in the streamwise direction is positive just downstream from the point of tangency of the nose with the conical section (see fig. 4) and hence tends to thicken the boundary layer and promote transition. Both the schlieren pictures and the force measurements indicate that for the high Reynolds numbers the boundary layer is turbulent over a much greater portion of the surface of the blunter of the two bodies. This result is in agreement with what might be expected on the basis of the differences in the pressure distributions for the two models. Although the adverse gradients for both the $d/D=0.30$ and $d/D=0.50$ models start at essentially the same longitudinal station along the models, and initially are of approximately equal magnitude, the adverse gradient for the blunter model, $d/D=0.50$, extends over most of the conical section of the model; whereas the gradient for the $d/D=0.30$ model is neutral over most of the conical section. Hence, it appears reasonable to expect a lower Reynolds number of transition for the blunter of the two models.

For the $d/D=0.30$ and $d/D=0.50$ models at Mach numbers of 1.24 and 1.44, equation (2) yields values of the wave drag alone which are even greater than the measured foredrags at the lower Reynolds numbers. This discrepancy is attributed to the fact that at these Mach numbers the empirical expression includes too large a value for the wave drag of the hemispherical portion of these models. (See fig. 5.) Hence, for the foredrag estimates shown in figure 8 for Mach numbers 1.24 and 1.44, the lower values of the wave drag of the hemispherical portion of the models obtained from experiment (fig. 5) were used. For all other Mach numbers the empirical expression (eq. (2)) was used. The estimated foredrag results obtained are in fair agreement with the experimental data.

As previously discussed, preliminary estimates and experiment have both shown that a small saving in foredrag may be achieved through the use of a hemispherically blunted cone in place of a sharp cone of the same fineness ratio. Although this type of blunting can be beneficial, preliminary estimates have also indicated that no drag reduction can be achieved by simply replacing the sharp nose of a given cone with a hemispherical tip. In this case the cone angle is not reduced, since the length of the model is reduced instead. In order to verify these results, tests have been made at Mach numbers 1.44 and 1.99 for a series of hemispherically blunted cones, formed by progressively blunting an $L/D=3$ cone. Both the experimental foredrag results and the estimated values of foredrag are plotted in figure 10. It is evident from the figure that there is good agreement between experiment and theory, and that, as expected, there is no drag reduction due to mere blunting of the parent cone.

THEORETICAL MINIMUM DRAG NOSE SHAPES

Comparison of experimental and theoretical foredrag.—Comparisons of the experimental and theoretical foredrag variations with Mach number for the theoretical minimum drag noses, the $L/D=3$ cone and the L-V ogive, are shown in figure 11. The theoretical drag calculations have been

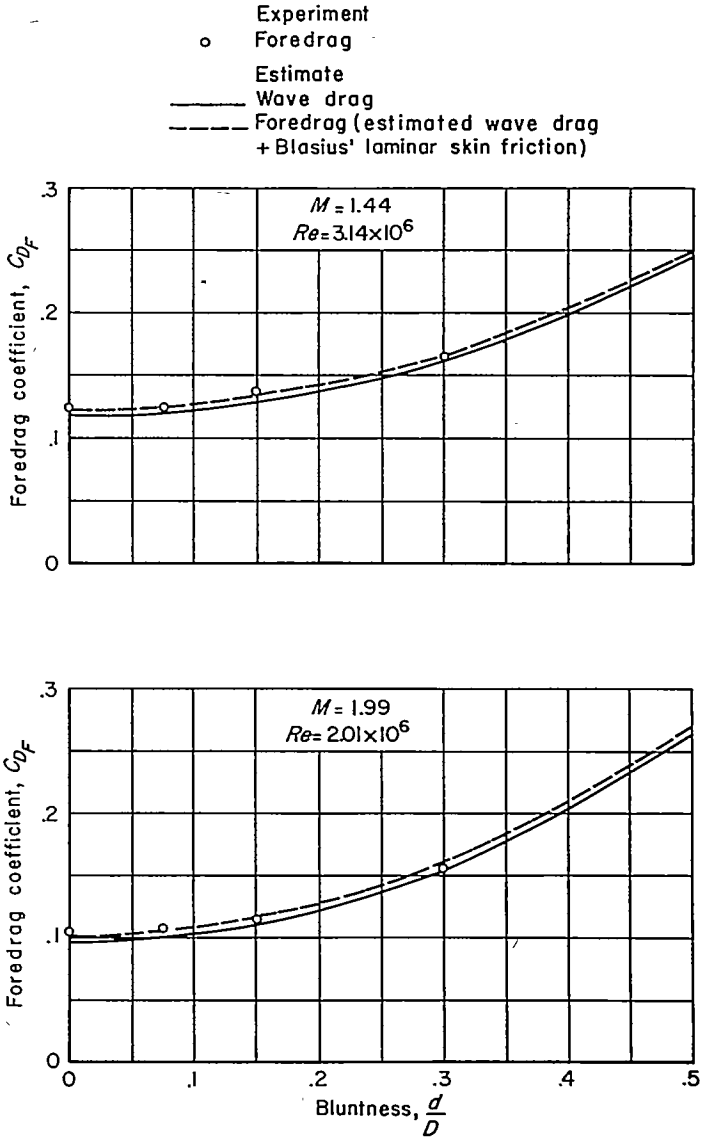

FIGURE 10.—Variation of foredrag coefficient with bluntness for hemisphere-cone series, constant cone angle=18°56′.

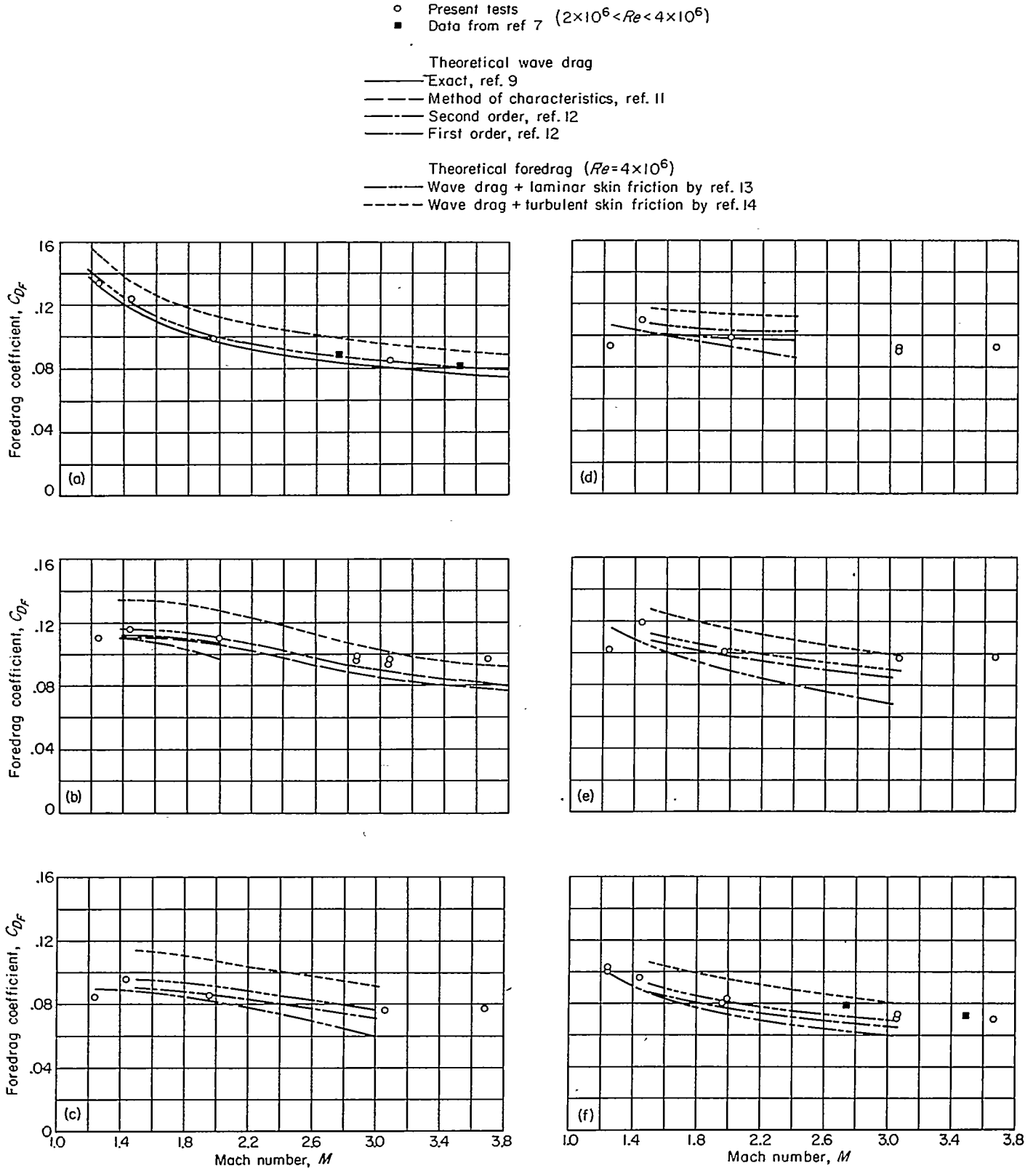

(a) Model No. 1, cone, $\frac{L}{D}=3$.

(b) Model No. 16, L–V Ogive, $\frac{L}{D}=2.93$.

(c) Model No. 13, L–D Haack, $\frac{L}{D}=3$.

(d) Model No. 14, L–V Haack, $\frac{L}{D}=3$.

(e) Model No. 15, D–V Haack, $\frac{L}{D}=3$.

(f) Model No. 10, Hypersonic Opt., $\frac{L}{D}=3$.

FIGURE 11.—Comparison of experimental and theoretical foredrag for various models.

limited in most cases to a smaller Mach number range than that for which experimental results are available. For Mach numbers less than 1.4 or greater than about 3, the conical tip approximations to the true body shapes which would have been necessary for application of the perturbation theory to the minimum drag shapes were considered unreasonably large; hence, the second-order theoretical results were limited to Mach numbers between 1.4 and 3. In fact, for the *L-V* Haack nose the theoretical calculations were limited to Mach number 2.4, as an excessive amount of conical tip modification would be necessary for the theory to be applicable at higher Mach numbers. Theoretical estimates of the foredrag have been made by the addition of flat-plate skin-friction values to the computed wave drag, the skin friction being calculated for a Reynolds number of 4×10^6. Although some of the experimental data were taken at lower Reynolds numbers (between 2×10^6 and 4×10^6), the error introduced by calculation of the skin friction at one Reynolds number is small and certainly well within the accuracy of the experimental results. Either completely laminar (ref. 13) or completely turbulent (ref. 14) skin-friction drag has been assumed, although the schlieren pictures indicated that for the tests at Mach numbers of 3.06 and 3.67 boundary-layer transition occurred on some of the models.

A comparison of the experimental and theoretical foredrag for the $L/D=3$ cone has been included in figure 11, since such a comparison indicates how well the skin-friction drag may be calculated and also provides an indication of the accuracy of the other experimental results. For the Reynolds numbers of this investigation, schlieren observations indicated laminar-boundary-layer flow on the cone at all Mach numbers. The foredrag of the cone was closely estimated by the addition of the exact Taylor-Maccoll wave drag and Blasius' incompressible laminar skin friction.[5]

In general, good agreement between the experimental and theoretical foredrag for laminar-boundary-layer flow was obtained for most of the models at Mach numbers of 1.4 and 2.0. Nevertheless, at Mach number 2 the foredrag of the *L-D* and *L-V* Haack shapes are overestimated by about the magnitude of the theoretical laminar-skin-friction drag. For a Mach number of 3 the foredrag of the cone and the foredrag of the *L-D* Haack shape are in good agreement with the theory for laminar-boundary-layer flow. However, the comparisons indicate that the boundary-layer flow for the *L-V* ogive, the *D-V* Haack shape, and the hypersonic optimum shape were at least partially turbulent at this Mach number. At the maximum Mach number ($M=3.67$) the experimental foredrag of the *L-V* ogive exceeds even the theoretical value for completely turbulent boundary-layer flow. This same result is also inferred from the comparison for the *D-V* model. It is not clear which part of the theoretical foredrag is at fault, that is, the wave drag or the skin-friction drag. However, it appears most likely that the theoretical-skin-friction drag is too small, since considerable confidence may be placed in the wave drag value, particularly for the *L-V* ogive.[6]

The data also show that for these particular body shapes, the first-order theory yields acceptable values of wave drag for Mach numbers close to 1.4 only. At the higher Mach numbers, the first-order theory yields results which are too low.

Although slender-body theory has sometimes been used to calculate the wave drag of shapes with fineness ratios as low as these, the wave drag coefficients of 1/9, 1/8, and 1/6 for the *L-D*, *L-V*, and *D-V* Haack shapes (ref. 2), respectively, are too large at all Mach numbers as compared with the results in figures 11(c), 11(d), and 11(e).

Comparison of foredrag of theoretical minimum drag nose shapes with foredrag of other nose shapes.—In order to assess the theoretical minimum drag shapes for the three auxiliary conditions of given length and diameter, given length and volume, or given diameter and volume, other common shapes with identical values of these parameters have been tested and comparisons of the results are shown in figure 12. Although the Reynolds number was not constant throughout the Mach number range, it was unchanged for all the tests at each Mach number. Hence, differences in foredrag between models compared at a given Mach number may not be attributed to differences in Reynolds number.

The foredrag coefficients of the theoretical minimum drag shapes for a given length and diameter, the *L-D* Haack nose (or Kármán ogive), and the hypersonic optimum nose (¾ power and Ferrari shape, see fig. 2) are compared with the foredrag coefficients of the parabolic nose in figure 12(a). It is noteworthy that the *L-D* Haack nose is not the least-drag shape for any Mach number within the range of the tests. For the major portion of the Mach number range (above Mach number 1.5), the hypersonic optimum shape has the least foredrag. It is somewhat surprising that an optimum shape based upon Newtonian impact theory should have less drag than the *L-D* Haack nose at these relatively low supersonic Mach numbers. It is not clear whether this anomaly results from the restriction of zero slope at the base which was evidently assumed in the derivation of the *L-D* Haack nose, or whether this is a result of the low fineness ratio of the models. To investigate this latter point, the wave drag coefficients of both the *L-D* Haack and the hypersonic optimum shapes were calculated by second-order theory for fineness ratios of 3, 5, and 7 at a Mach number of 3. These results (fig. 13) show that the wave drag coefficient of the "Haack" shape is the larger for fineness ratios of 3 and 5. For fineness ratio 7 any difference in wave drag between the *L-D* Haack and the hypersonic optimum shapes is so small as to be within the limits of uncertainty of the calculations. To provide a better indication of the combinations of Mach number and fineness ratio for which the hypersonic optimum nose has less wave

[5] The Handtzahe and Wendt transformation of laminar-boundary-layer skin-friction drag of a flat plate to that of a cone was neglected since its inclusion would have increased the foredrag by only 1 percent.

[6] The foredrag values reported herein for the *L-V* ogive ($L/D=2.93$) are about 10 percent lower than those reported in reference 7 for an $L/D=3$ ogive, although the foredrag results for the cone and hypersonic optimum shapes (figs. 11 (a) and 11 (f)) are in agreement. Even though the tests have been rerun and the data have been carefully checked, no satisfactory explanation has, as yet, been found for this difference.

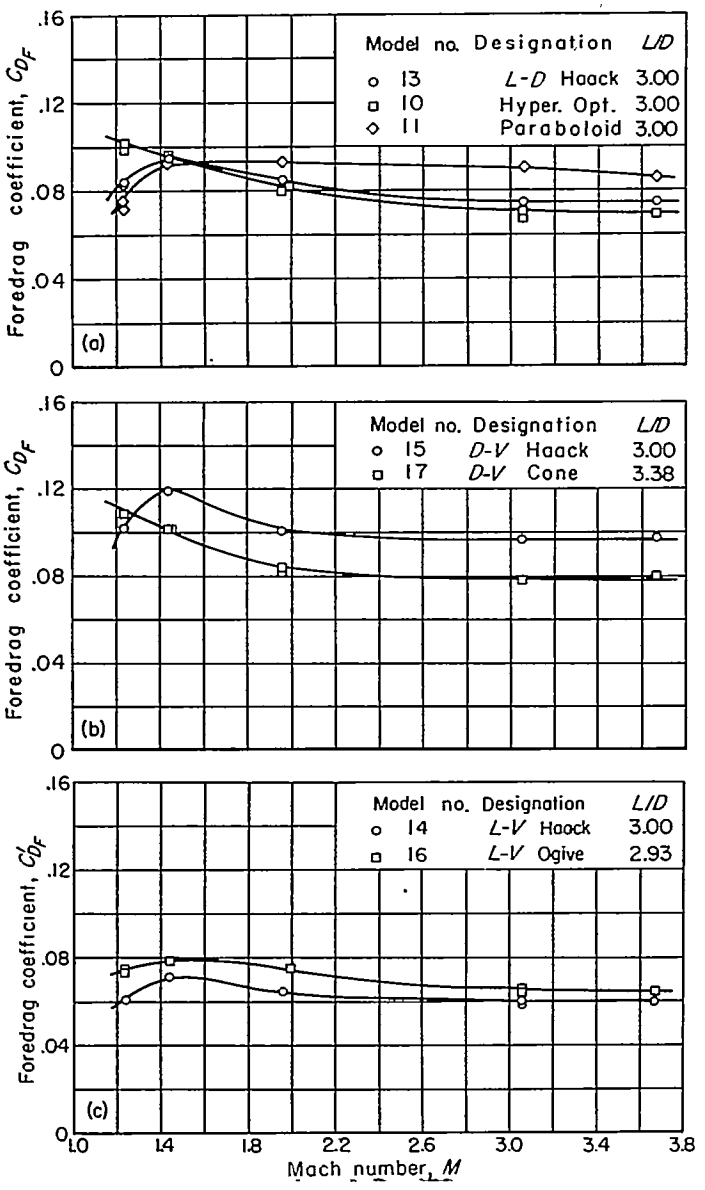

(a) Length and diameter given.
(b) Diameter and volume given.
(c) Length and volume given.

FIGURE 12.—Comparison of foredrag of Haack models with other models having the same two specified parameters.

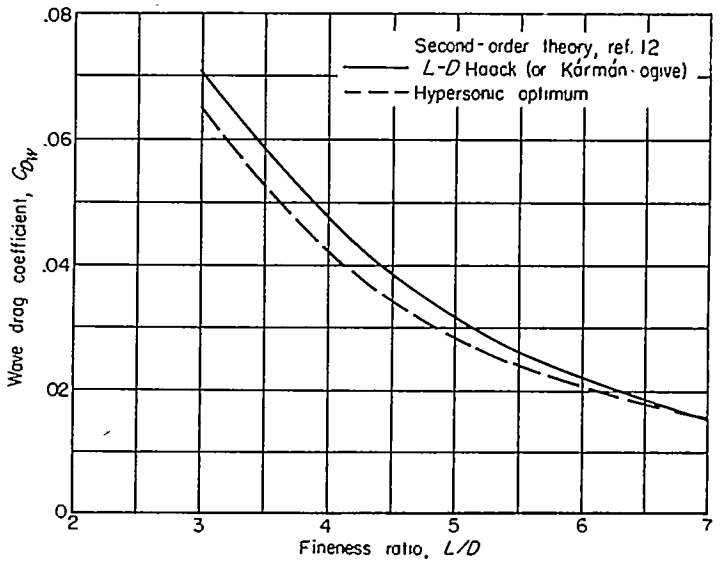

FIGURE 13.—Variation of wave drag coefficient with fineness ratio for the theoretical minimum drag nose shapes of specified length and diameter at Mach number 3.

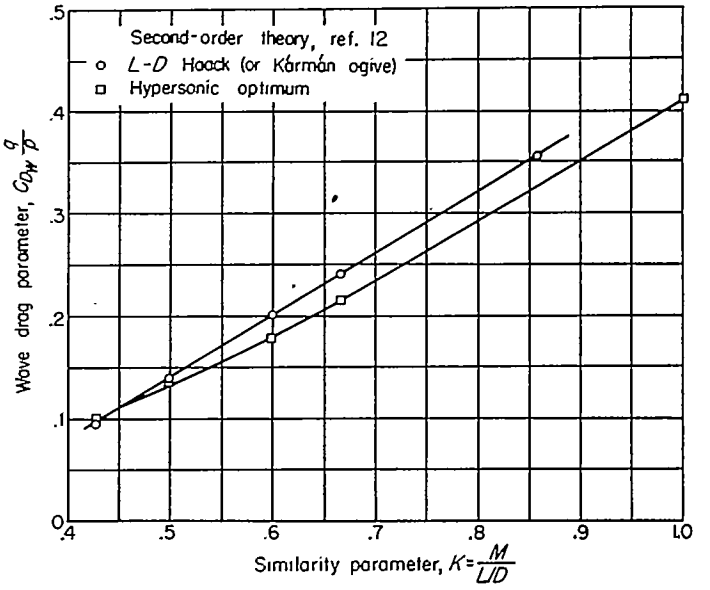

FIGURE 14.—Variation of wave drag parameter, $C_{D_W}\frac{q}{p}$, with the similarity parameter for the theoretical minimum drag nose shapes of specified length and diameter.

drag than the *L-D* Haack nose, the results of all of the available second-order solutions for these shapes have been plotted in figure 14. The plot is made in terms of the hypersonic similarity parameter, $K=M/(L/D)$, and indicates that for values of K in excess of about 0.4 or 0.5 the hypersonic optimum shape has the lower wave drag.

The foredrag of the theoretical minimum drag shape for a given diameter and volume (*D-V* Haack, model 15) is compared in figure 12(b) with the foredrag of a cone (*D-V* cone, model 17) having identical values of diameter and volume. Except for Mach numbers below about 1.4, the foredrag of the cone is of the order of 20 percent lower than that of the theoretical optimum shape. Again, this result may be due either to the low fineness ratio of the bodies tested or the failure of the slender-body theory to predict the correct minimum drag shape for all possible shapes rather than the correct minimum drag shape for bodies with zero slope at the base. In any event, it could be expected that the drag difference would be much less for higher fineness ratio noses.

The foredrag of the theoretical minimum drag shape for a given length and volume (*L-V* Haack, model 14) is compared in figure 12(c) with the foredrag of a circular-arc ogive (*L-V* ogive, model 16) having identical values of length and volume. Since the base areas of these noses differ, the foredrag coefficients are based on $(\text{volume})^{2/3}$ instead of base area in order that a direct comparison of the foredrags may be conveniently made. Over the complete Mach number range the foredrag coefficient of the *L-V* Haack model is between 8 and 16 percent lower than the foredrag coefficient of the *L-V* ogive. For both models the variation of foredrag coefficient with Mach number is similar.

Foredrag of nose shapes defined by $r=R(X/L)^n$.—In reference 7 foredrag results of fineness ratio 3 models for $n=1$, $\frac{3}{4}$, $\frac{1}{2}$, and $\frac{1}{4}$ are presented for the Mach number range of 2.73 to 5.00 and for length Reynolds numbers between 2×10^6 and 3×10^6. In the present investigation similar models have been tested at Mach numbers from 1.24 to 3.67 and Reynolds numbers between 2×10^6 and 4×10^6 in order to extend the Mach number range of available drag data. The foredrag results of this investigation are presented in figure 15 and are compared with part of the results of reference 7, replotted for the overlapping Mach number

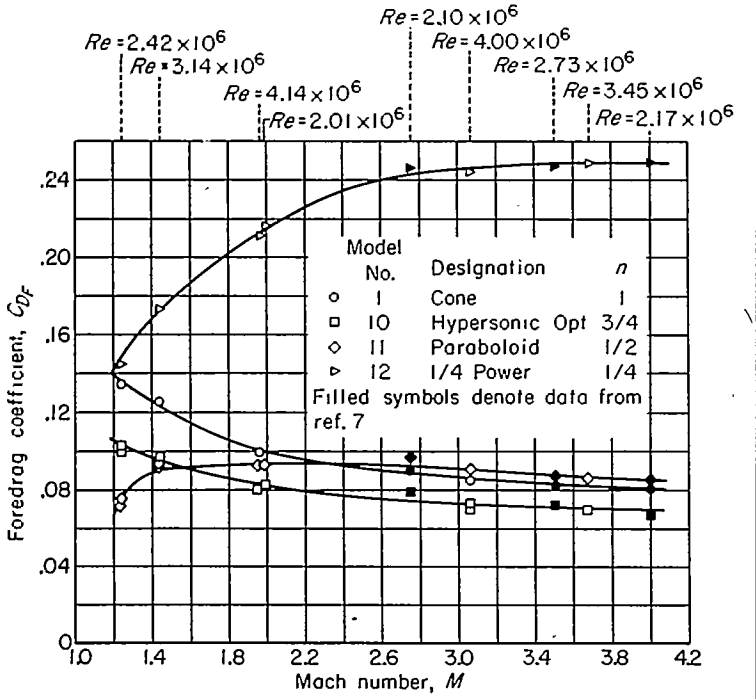

FIGURE 15.—Variation of foredrag coefficient with Mach number for the family of $\frac{L}{D}=3$ nose shapes defined by $r=R\left(\frac{X}{L}\right)^n$.

range of both investigations. In general, there is good agreement between the data from both sources, although there are small differences which may be attributed to variations in Reynolds number. Both the hypersonic optimum nose ($n=\frac{3}{4}$) and the conical nose ($n=1$) show a similar decrease in foredrag coefficient with increase in Mach number over the complete Mach number range. The hypersonic optimum nose, however, has much the lower foredrag (about 24 percent lower at Mach number 1.24 and 15 percent lower at Mach number 3.67). In contrast with the decrease in the foredrag coefficient with increasing Mach number for the hypersonic optimum and conical noses, the foredrag coefficients for the parabolic and $\frac{1}{4}$-power noses increase with increasing Mach number in the lower part of the Mach number range.

COMPARISON OF FOREDRAG OF ALL THE FORCE MODELS

In figure 16 a comparison of the variation of foredrag coefficient with Mach number for all the force models tested is shown. In general, it is seen that for the more blunt noses (models 5, 12, and 18) the foredrag coefficient increases with increase in Mach number, while for the other noses the foredrag coefficient decreases with increase in Mach number over most of the range. It is of interest to note that the ellipsoid (model 18), although showing a large increase in foredrag coefficient with increase in Mach number to Mach number 2, has constant foredrag coefficient for Mach numbers above 2. There is no minimum drag nose for the complete Mach number range, although the hypersonic optimum nose (model 10) has the least drag for Mach numbers above 1.5. Below Mach number 1.5 the paraboloid (model 11) has the lowest drag, slightly less than the drag of the *L–D* Haack nose (model 13). Of special note is the observation that many of the nose shapes have less drag than the cone (model 1), particularly at the lower Mach numbers.

CONCLUSIONS

Drag measurements at zero angle of attack have been made for various hemispherically blunted cones, theoretical minimum drag nose shapes, and other more common profiles of fineness ratio 3. An analysis of the results for a Mach number range of 1.24 to 7.4 and for Reynolds numbers between 1.0×10^6 and 7.5×10^6 has led to the following conclusions:

1. No model had the least foredrag for the complete Mach number range.
2. Of the models tested the paraboloid of revolution had the least foredrag below a Mach number of 1.5, and the hypersonic optimum shape had the least foredrag above a Mach number of 1.5.
3. The theoretical shapes for minimum pressure drag derived by von Kármán and by Haack for given length and diameter or given diameter and volume do not have less drag than all other possible shapes having identical values of the same parameters.
4. For the hemispherically blunted cones of low fineness ratios (of the order of 3):
   a. Small reductions in foredrag may be achieved by hemispherical blunting (hemisphere diameter approximately 15 percent of base diameter) if the fineness ratio is held constant and, hence, the cone angle reduced with increased blunting. If the cone angle is held constant and the fineness ratio reduced, hemispherical blunting results in increased foredrag.
   b. A relatively large hemispherical tip diameter (as large as 30 percent of the base diameter at Mach numbers of 1.24 and 1.44) may be used without increasing the drag above that of a sharp-nosed cone of the same fineness ratio.
   c. For large spherical bluntnesses (nose diameters of the order of 50 percent of the base diameter) drag penalties were moderate at Mach numbers less than 1.5 but became severe with increasing Mach number.
   d. For Mach numbers of 2 and greater the wave drag may be accurately estimated by the addition of the wave drag of the hemispherical tip calculated from an empirical expression and the wave drag of the conical portion from Taylor-Maccoll theory.

AMES AERONAUTICAL LABORATORY,
NATIONAL ADVISORY COMMITTEE FOR AERONAUTICS,
MOFFETT FIELD, CALIF., *Aug. 28, 1952.*

Model	No	Designation	d/D	L/D
○	1	Hemisphere-Cone,	0.000	3.00
□	2	Hemisphere-Cone,	.075	3.00
◇	3	Hemisphere-Cone,	.150	3.00
▷	4	Hemisphere-Cone,	.300	3.00
▽	5	Hemisphere-Cone,	.500	3.00
▽	7	Hemisphere-Cone,	.075	2.81
▷	8	Hemisphere-Cone,	.150	2.62
◇	9	Hemisphere-Cone	.300	2.24

Model	No	Designation	L/D
◇	10	Hyper. Opt	3.00
▷	11	Paraboloid	3.00
●	12	1/4 Power	3.00
■	13	L-D Haack	3.00
◆	14	L-V Haack	3.00
▶	15	D-V Haack	3.00
▼	16	L-V Ogive	2.93
▼	17	D-V Cone	3.38
▽	18	Ellipsoid	3.00

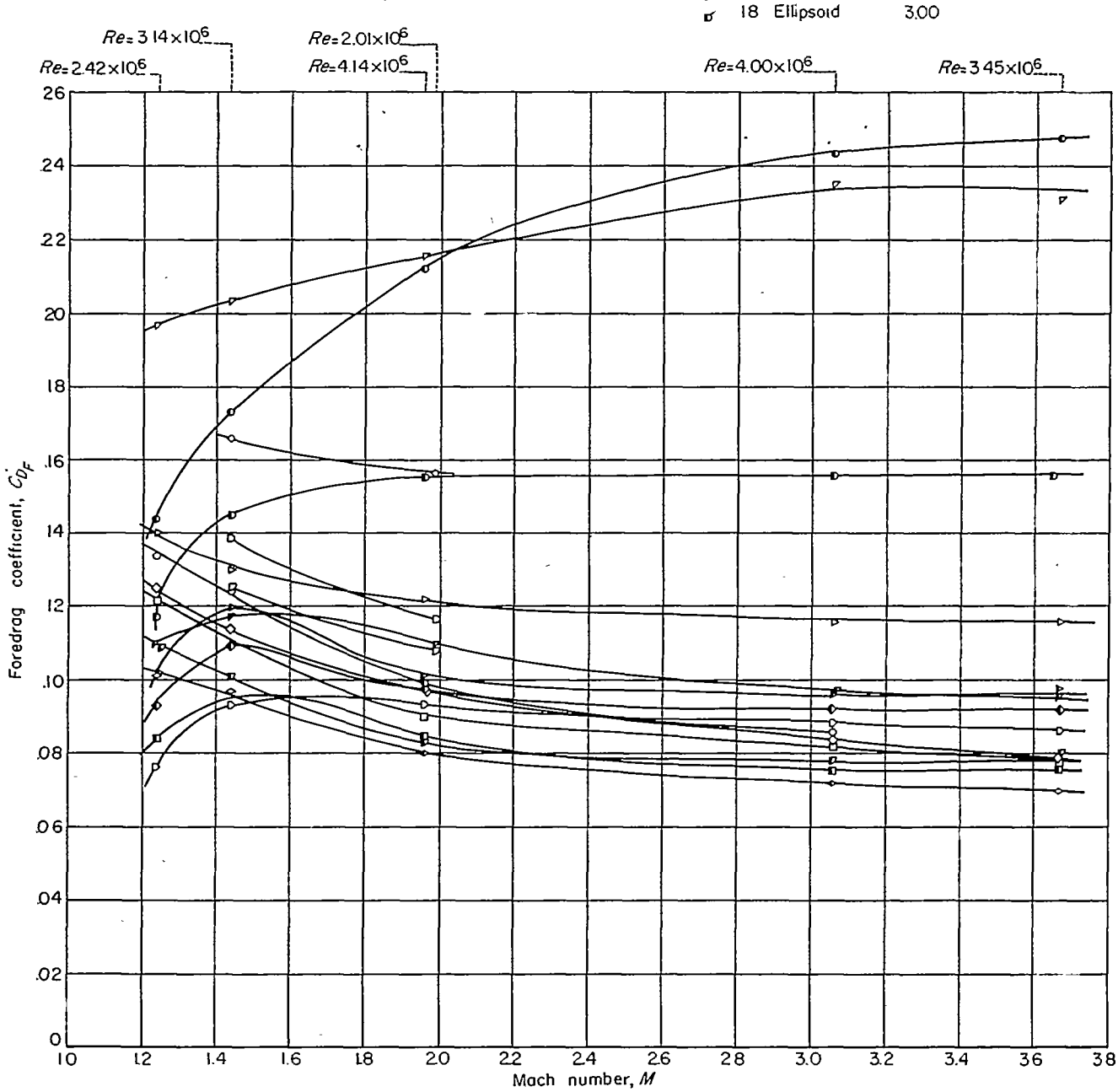

FIGURE 16.—Variation of foredrag coefficient with Mach number for all the force models tested.

REFERENCES

1. von Kármán, Th.: The Problems of Resistance in Compressible Fluids. R. Accad. d' Italia, Cl. Sci. Frs. Mat. e Nat., vol XIV, 1936, pp. 222–276. (Fifth Volta Congress held in Rome, Sept. 30–Oct. 6, 1935).
2. Haack, W.: Projectile Forms of Minimum Wave Resistance. (Translation) Douglas Aircraft Company, Inc., Rep. 288, 1946.
3. Lighthill, M. J.: Supersonic Flow Past Bodies of Revolution. R. & M. No. 2003, British A. R. C., 1945.
4. Sears, William R.: On Projectiles of Minimum Wave Drag. Quart. Appl. Math., vol. IV, no. 4, Jan. 1947, pp. 361–366.
5. Ward, G. N.: Supersonic Flow Past Slender Pointed Bodies. Quart. Jour. Mech. and Appl. Math., vol. II, pt. 1, March 1949, pp. 75–99.
6. Ferrari, Carlo: The Body and Ogival Contour Giving Minimum Wave Drag. Atti dell Accademia delle Scienze di Torino, vol. 84, no. 1, pp. 3–18, 1949–50. (Translated by R. H. Cramer, Cornell Aero. Lab., Inc., Buffalo, New York, presented at session of Reale Accademia delle Scienze di Torino, Nov. 23, 1949.
7. Eggers, A. J., Jr., Resnikoff, Meyer M., and Dennis, David H.: Bodies of Revolution for Minimum Drag at High Supersonic Airspeeds. NACA Rep. 1306, 1957 (Supersedes NACA TN 3666).
8. Seiff, Alvin: A Free-Flight Wind Tunnel For Aerodynamic Testing at Hypersonic Speeds. NACA Rep. 1222, 1955 (Supersedes NACA RM A52A24).
9. Mass. Inst. of Tech., Dept. of Elect. Engr., Center of Analysis. Tables of Supersonic Flow Around Cones, by the Staff of the Computing Section, Center of Analysis, under the direction of Zdenek Kopal. Tech. Rep. No. 3, Cambridge, 1949.
10. Stewart, H. J.: The Theoretical Lift and Drag of Cones at Supersonic Speeds. Jet Propulsion Lab., GALCIT Memo. No. 4–14, Nov. 18, 1946.
11. Ehret, Dorris M., Rossow, Vernon J., and Stevens, Victor I.: An Analysis of the Applicability of the Hypersonic Similarity Law to the Study of Flow About Bodies of Revolution at Zero Angle of Attack. NACA TN 2250, 1950.
12. Van Dyke, Milton D.: Practical Calculation of Second-Order Supersonic Flow Past Nonlifting Bodies of Revolution. NACA TN 2744, 1952.
13. Blasius, H.: Grenzschichten un Fliissigkeiten mit kleiner Rubung. Zx. Math. un. Phys. Bd 56, p. 1 (1908).
14. Rubesin, Morris W., Maydew, Randall C., and Varga, Steven A.: An Analytical and Experimental Investigation of the Skin Friction of the Turbulent Boundary Layer on a Flat Plate at Supersonic Speeds. NACA TN 2305, 1951.
15. Grimminger, G., William, E. P., and Young, G. B. W.: Lift on Inclined Bodies of Revolution in Hypersonic Flow. Jour. Aero. Sci., vol. 17, no. 1, November 1950, pp. 675–690.
16. Hodges, A. J.: The Drag Coefficient of Very High Velocity Spheres. Jour. Aero. Sci., vol. 24, no. 10, Oct. 1957, pp. 755–758.
17. Hart, Roger G.: Flight Investigation of the Drag of Round-Nosed Bodies of Revolution at Mach Numbers From 0.6 to 1.5 Using Rocket Propelled Test Vehicles. NACA RM L51E24, 1951.
18. Vincenti, Walter G., and Wagoner, Cleo B.: Transonic Flow Past a Wedge Profile with Detached Bow Wave. NACA TN 2339, 1951. NACA Rep. 1095, 1953 (Supersedes NACA TN's 2339 and 2588).
19. Jack, John R., and Gould, Lawrence I.: Aerodynamics of Slender Bodies at Mach Number of 3.12 and Reynolds Numbers from 2×10^6 to 15×10^6. II-Aerodynamic Load Distributions of Series of Five Bodies Having Conical Noses and Cylindrical Afterbodies. NACA RM E52C10, 1952.